National Conference on Recent Advances in Engineering, Technology, Science, Management and Humanities (NCRAETSMH – 2025)

23rd February, 2025, Nagpur, Maharashtra, India.

CERTIFICATE NO : NCRAETSMH /2025/C0225140

High-Performance Magnetic Hyperthermia Using Hydrothermally Treated Superparamagnetic Iron Oxide Nanoparticles

Soumen Mondal

Research Scholar, Department of Physics, Mansarovar Global University, Sehore, M.P., India.

ABSTRACT

The goal of this research is to create magnetic hyperthermia agents with enhanced performance by using hydrothermally treated SPIONs. In order to increase the heating efficiency, stability, and biocompatibility of SPIONs for possible use in biomedicine, they were synthesized and their physicochemical and magnetic characteristics were enhanced using the hydrothermal treatment approach. To get the desired magnetic properties, high crystallinity, and uniform particle size, the synthesis required careful regulation of variables such precursor concentration, temperature, and pressure. In the Physical Laboratory, we characterized the prepared nanoparticles. In collaboration with other university laboratories, we performed additional tests, such as structural analysis, surface functionalization assessment, and in vitro heating performance (specific absorption rate, SAR). In comparison to their untreated counterparts, SPIONs that were hydrothermally treated showed much higher SAR values and better magnetic characteristics, suggesting that they might be used more effectively in magnetic hyperthermia applications. Confirming their appropriateness for application in biomedicine, the team went on to examine the nanoparticles' colloidal stability and biocompatibility in physiological settings. Future in vivo investigations and clinical translation may build on this work, which offers crucial insights into the function of hydrothermal treatment in optimizing SPIONs for safe, effective, and targeted magnetic hyperthermia cancer therapy.

Keywords: - Magnetic, Nanoparticles, Superparamagnetic, Hydrothermal, Iron Oxide.

1. INTRODUCTION

Magnetic hyperthermia is a relatively new and exciting therapeutic strategy for cancer treatment, especially when used in conjunction with more traditional methods like radiation and chemotherapy. By exposing magnetic nanoparticles to an alternating magnetic field (AMF), this technique may selectively raise the temperature of tumor tissues, usually to a range of 41°C to 46°C, using the heat they produce. The therapeutic index may be improved and systemic adverse effects minimized by inflicting permanent damage on cancer cells by a controlled temperature increase, while surrounding healthy tissues are spared. Due to their advantageous magnetic characteristics, ease of surface modification, chemical stability, and great biocompatibility, superparamagnetic iron oxide nanoparticles (SPIONs) have garnered substantial interest among the different materials studied for magnetic hyperthermia applications. Hyperthermia applications rely on superparamagnetic. Because SPIONs do not retain their magnetization even after an external magnetic field is removed, they are far less likely to aggregate particles and are more biocompatible than ferromagnetic materials. Generally speaking, processes like Brownian and Néel relaxation control the heat generation capability of SPIONs in the presence of an alternating magnetic field. Particle size, shape, magnetic characteristics, and colloidal stability are among the many variables that significantly affect the specific absorption rate (SAR), a measurable metric of heating efficiency. To enhance the therapeutic effectiveness, it is vital to carefully manage the synthesis and post-synthesis treatment of nanoparticles.

In order to improve the physicochemical and magnetic characteristics of SPIONs, hydrothermal treatment has lately been a popular post-synthesis technique. An improved control over particle size distribution, crystallinity, surface structure, and phase purity may be achieved by crystallizing iron oxide nanoparticles in a high-temperature and high-pressure aqueous environment. To optimize magnetic performance and heat production under an alternating magnetic field, hydrothermal treatment is preferable to traditional methods like thermal decomposition or co-precipitation because it produces materials with better crystallinity and more uniform morphology. To further tune the magnetic and biological characteristics, the technique also allows for the insertion of other dopants or surface functional groups. Maintaining an optimal ratio of particle size to magnetic characteristics is a key issue in developing high-performance magnetic hyperthermia. It is important to minimize particle aggregation and ensure safe biological use with bigger particles, but they run the danger of losing their superparamagnetic activity, even though larger particles often have stronger magnetic moments and better heating efficiency. The optimal conditions for maximizing SAR without sacrificing superparamagnetic are met by hydrothermally treated SPIONs, which have a high crystallinity and a regulated particle size distribution. By adjusting synthesis parameters including precursor concentration, reaction time, temperature, and pressure, one may fine-tune the nanoparticle properties for maximum efficiency.

Hydrothermal treatment of SPIONs normally improves their colloidal stability in physiological conditions and also improves their magnetic characteristics. To guarantee uniform nanoparticle dispersion, low aggregation, and extended circulation duration, colloidal stability is critical for intravenous delivery. To further improve biocompatibility and provide active targeting capabilities, surface functionalization is crucial, which is often accomplished during or after hydrothermal treatment. One way to enhance in vivo stability, decrease opsonization, and avoid fast clearance by the reticuloendothelial system is to encapsulate nanoparticles with biocompatible polymers like dextran or polyethylene glycol (PEG). Under certain field strength and frequency circumstances, the intrinsic loss power (ILP) or surface area ratio (SAR) is usually used to assess the heating efficacy of SPIONs in biological applications. To generate therapeutic temperatures with smaller dosages of nanoparticles, thereby avoiding possible toxicity, high SAR values indicate efficient heat production. Recent research has shown that SPIONs may reach much better SAR values after being hydrothermally treated than untreated ones. This shows how important the post-synthesis procedure is for improving the hyperthermia effectiveness of the material. With increased tumor ablation effectiveness and less systemic toxicity in preclinical studies, these nanoparticles have shown encouraging in vitro and in vivo outcomes. Accurately targeting the tumor location with nanoparticle delivery is another key component of magnetic hyperthermia. Active targeting via surface conjugation of ligands like antibodies, peptides, or aptamers is one common targeting strategy, whereas passive targeting is based on the increased permeability and retention (EPR) effect. Because of their large surface area and well-defined surface chemistry, hydrothermally treated SPIONs provide a strong foundation for functionalization. Incorporating targeting moieties in this way improves hyperthermia results by allowing for effective accumulation at the tumor location without drastically altering magnetic characteristics or colloidal stability.

There are still a number of obstacles to overcome before SPION-based hyperthermia that has been hydrothermally treated may be used in therapeutic settings, notwithstanding these developments. A major concern is the possibility of chronic toxicity and the buildup of nanoparticles in vital organs like the spleen and liver. While SPIONs have the potential to break down into iron ions that the body can use for metabolism, there is still a need for further research on their long-term biodistribution and clearance. Moreover, an essential part of clinical translation is adjusting the magnetic field characteristics (frequency and amplitude) within acceptable biological limits while keeping the heating performance efficient. The need for repeatability, scalability, and comprehensive characterization of every manufacturing batch is emphasized by regulatory issues, which also play a substantial role in nanoparticle design. A state-of-the-art method in cancer treatment is high-performance magnetic hyperthermia that employs superparamagnetic iron oxide nanoparticles that have been hydrothermally processed. Hydrothermally treated SPIONs provide a promising platform for therapeutic heat generation under alternating magnetic fields because to their increased magnetic characteristics, greater colloidal stability, and functionalization capabilities. To make this technology even safer and more effective, researchers are always looking for ways to tweak the synthesis settings, surface treatments, and targeting tactics.

2. REVIEW OF LITERATURE

Pucci, Carlotta et al., (2022). Because of their capacity to induce hyperthermia in reaction to a reversed magnetic field, superparamagnetic iron oxide nanoparticles (SPIONs) have garnered interest from the biomedical community. Particularly in tumor cells, which appear to be more sensitive to temperature increases, hyperthermia is known to induce cell death. This is why using heat to treat cancer has gained some traction. Although this method shows promise, there is currently a lack of information regarding the molecular effects of magnetic hyperthermia and the specific cell death pathways it triggers. However, therapeutic results and clinical translation could be enhanced with a thorough understanding of this component. In addition, much research over the past two decades has focused on developing delivery strategies to enhance SPION bio distribution and localization at the action site. Recent in vitro and in vivo studies have proposed potential cell death pathways activated by the treatment, and this review aims to give a general outline of magnetic hyperthermia, with a focus on iron oxide nanoparticles and their interactions with magnetic fields, as well as new strategies to efficiently deliver them to the target site. We will also go over their present health state and talk about how omics has helped us comprehend the molecular relationships between biological environments and iron oxide nanoparticles.

Dulińska-Litewka, Joanna et al., (2019). The medical sciences have been impacted by the rapid growth of nanotechnology in recent times. One such example is SPIONs, or superparamagnetic iron oxide nanoparticles. The superparamagnetic characteristics of SPIONs have led to their use in magnetic hyperthermia and magnetic resonance imaging (MRI). Since SPIONs, in contrast to bulk iron, do not retain any magnetization when exposed to an external magnetic field, their behavior can be precisely controlled from a distance. For this reason, they can be an integral part of cutting-edge medication delivery systems. Due to its facile production, biocompatibility, multifunctionality, and ability of future surface modification with various chemical agents, SPIONs could benefit several disciplines of medicine. The significant absorption of SPIONs by macrophages is one of their drawbacks. Still, they show a lot of promise in cancer treatment, according to the current research. This is particularly true for brain, breast, prostate, and pancreatic malignancies. Our research aims to provide an overview of SPIONs, their basic features, their current medical role, and their applications in the hopes that this may encourage the development of better SPION systems in the future.

Pala, Jay. (2017) Modern medicine has made great strides in the detection and treatment of cancer, but the disease still ranks high among the leading killers. The use of engineered nanoparticles in cancer detection and treatment might be game-changing. When it comes to cancer treatment using magnetic hyperthermia, the most promising candidate has been superparamagnetic iron oxide nanoparticles, or SPIONs. Medications can be delivered to cells at a higher concentration when iron oxide super paramagnetic nanoparticles are used. Iron oxide nanoparticles' one-of-a-kind characteristics have made it possible to circumvent cancer treatment's drawbacks, such as the potentially fatal radiation dosage and undesirable side effects. Recent improvements in treating magnetic hyperthermia with SPIONs have been discussed in this study.

Pala, Jay et al., (2017) Cancer is one of the leading killers in today's world, even with the most recent breakthroughs in detection and treatment. Nanoparticles that have been engineered could completely change how cancer is detected and treated. Among the several candidates for cancer treatment using magnetic hyperthermia, superparamagnetic iron oxide nanoparticles (SPIONs) have shown the most promise. An increase in the intracellular concentration of medications can be achieved through the use of iron oxide super paramagnetic nanoparticles. Overcoming the restrictions of cancer therapy, such as deadly radiation dosage and unpleasant side effects, has been made possible by the unique features of iron oxide nanoparticles. We have summarized the latest developments in the use of SPIONs to treat magnetic hyperthermia in this study.

3. MATERIALS AND METHODS

The physical laboratory conduct all of the tests required for this investigation. Additionally, other university labs conduct certain testing.

Chemicals And Reagents

Materials for the bimetallic Fe/Ni nanoparticles employed in this study include nickel nitrate, sodium borohydride, ferric chloride hexahydrate, nickel chloride, and iron sulfate. Propanol, acetone, ethanol, and kerosene oil were the solvents used. Preparation of kerosene oil samples containing Fe-Ni bimetallic nanoparticles for various uses We prepare the samples for flash points and fire points.

National Conference on Recent Advances in Engineering, Technology, Science, Management and Humanities (NCRAETSMH – 2025)

23rd February, 2025, Nagpur, Maharashtra, India.

We begin by preparing three separate solutions in 100 ml of kerosene oil: one with a concentration of 0 ppm, another with 30 ppm, and a third with 60 ppm. If you want to know how the nano catalyst affects flash and fire points, you may use an open tester cup to get the different values of your sample solutions. We use these metrics to assess the effect of bimetallic nanoparticles on the fuel efficiency of kerosene. Get your samples ready for cloud point and pourpoint analysis. By combining different amounts of the nano catalyst sample (0, 0.003 g, 0.006 g, 0.009 g) with 100 ml of kerosene gas, solutions with different concentrations (0 ppm, 30 ppm, 60 ppm, 90 ppm) were created for cloud and pour point measurements. The cloud point and pour point of the pure and modified kerosene fuel were examined to determine the effect of the nano catalyst. Collecting samples for calorimeter analysis. The calorific values are obtained by analyzing the water created by combustion reactions using a bomb calorimeter equipment. Use different amounts of nano catalyst (0, 0.0015 g, 0.003 g, 0.0045 g) in 50 ml of kerosene gas to prepare samples with different concentrations (e.g., 0 ppm, 10 ppm, 15 ppm, and 20 ppm).

We prepare the samples for the specific gravity test. Make a series of samples in 50 ml of kerosene oil with varying concentrations (0 ppm, 30 ppm, 60 ppm, 90 ppm) and varied weights (0.0015 g, 0.003 g, 0.0045 g). The effect of the nano catalyst on the specific gravity of the kerosene fuel will be confirmed. The ratio of sample mass to volume in 50 millilitres of kerosene oil is a good indicator of specific gravity. Acquiring kinematic viscosity characteristics from samples. A viscosity may be measured using an Ostwald viscometer. To determine the viscosity, dissolve a variety of samples in 500 ml of kerosene oil at several concentrations (0 ppm, 30 ppm, 60 ppm, 90 ppm): 0, 0.0015 g, 0.003 g, and 0.0045 g. We will investigate how the nano catalyst affects the fuel's viscosity. We can infer the amount of fuel effectiveness improved with the minuscule amount of the bimetallic nano catalyst from that parameter. The methylene blue dye degradation sample was prepared. Table 2 displays the ratios of dye solutions with varying catalyst concentrations, whereas Table 1 provides the ratios for preparing dye solutions with variable concentrations.

Table 1 Dye Solution Concentrations and Corresponding Properties

Dye concentration	Dye solution	Water
10 ppm	10 ml	90 ml
15 ppm	15 ml	85 ml
20 ppm	20 ml	80 ml

Table 2 Effect of Catalyst Concentration on Dye Solution Properties"

Dye concentration	Catalyst concentration	H2O2 concentration
20 ppm	0.20 mg mL^{-1}	2 ml
20 ppm	0.35 mg mL^{-1}	2 ml
20 ppm	0.50 mg mL^{-1}	2 ml

As shown in Table 3, the concentration of catalyst fluctuates in all solutions, whereas the concentration of dye and H2O2 stay constant.

Table 3 Effect of H_2O_2 Concentration on Dye Solution Properties

Dye concentration	Catalyst concentration	H2O2 concentration
20 ppm	0.20 mg mL^{-1}	1 ml
20 ppm	0.35 mg mL^{-1}	1 ml
20 ppm	0.50 mg mL^{-1}	1 ml

Engineering of Iron–Zinc Bimetallic Nanoparticles

The wet chemical approach was employed for the synthesis of Fe/Ni bimetallic nanoparticles, as previous nanoparticle preparation methods were found to be too expensive and difficult to control. Iron oxide and nickel nitrate salts were used as precursor materials in the wet chemical synthesis process. Initially, a solution was prepared by mixing 100 mL of ethanol/water (30:70 v/v) and 100 mL of distilled water containing sodium borohydride ($NaBH_4$) as the reducing agent, with ferric chloride hexahydrate ($FeCl_3 \cdot 6H_2O$) already added to the beaker. The mixture was thoroughly centrifuged with distilled water to remove excess $NaBH_4$. Next, 50 mL of ethanol was added to disperse the freshly formed iron nanoparticles, promoting the formation of bimetallic nanoparticles. Subsequently, 50 mL of ethanol solution containing nickel nitrate ($Ni(NO_3)_2$) was added, and the mixture was agitated for 30 minutes to ensure a uniform reaction. After the reaction, the nanoparticles were washed several times with a mixture of distilled water and ethanol to remove impurities. Finally, the resulting product was dried by heating at 120 °C for 24 hours.

Experimental Setup

The maximum absorbance of several concentrations of dye solution was measured in the 400–800 nm range using a UV-visible spectrophotometer (SP-300). The spectrophotometer was used to evaluate the ability of the bimetallic nanoparticles to degrade the organic dyes. XRD provides detailed information about the geometry and structural arrangement of the nanoparticles. Additionally, researchers at NTU employed scanning electron microscopy (SEM) to investigate the Fe/Ni morphology of the bimetallic nanoparticles. SEM images provided insights into the surface morphology of the nanoparticles. Furthermore, transmission electron microscopy (TEM) at the National Institute for Biotechnology and Genetic Engineering (NIBGE) was used to examine the morphology, chemical composition, size, shape, and internal structure of the Fe/Ni bimetallic nanoparticles. Compared to SEM images, TEM provided a clearer view of the nanoparticle shape and fine structural details.

Statistical analysis

All of the data was statistically analyzed using linear regression. In order to evaluate the relationship between different characterisation characteristics, regression models were used.

4. RESULTS AND DISCUSSION

To create bimetallic Fe/Ni nanoparticles, salts of iron and nickel have been used. The produced bimetallic Fe/Ni nanoparticles were examined using various methods. Lastly, experimental findings were obtained after carrying out several tests on the catalytic activity features of iron-zinc bimetallic nanoparticles.

XRD Characterization

The newly synthesized Fe/Ni bimetallic nano catalyst is characterized by the X-ray diffraction (XRD) pattern shown in Figure 1. The XRD results provide detailed information about the nanoparticle structure.

The sharp and well-defined peaks in the XRD pattern indicate that the material is highly crystalline, confirming the formation of well-structured nanoparticles. The presence of these specific diffraction peaks suggests that the nanoparticles possess cubic unit cells arranged in different orientations. Furthermore, the absence of additional peaks confirms the high purity of the sample, with no significant contaminant phases detected. An extra peak in the XRD pattern would indicate the presence of impurities, but no such peaks are observed.

The broadening of the diffraction peaks suggests that the particle size is in the nanometre range, with most particles estimated to be below 100 nm according to the Scherrer equation.

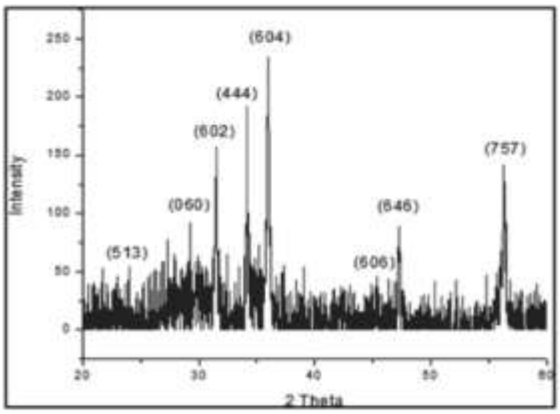

Figure 1 XRD Pattern of Synthesized Fe/Ni Bimetallic Nanoparticles

Figure 2 shows that the chemical composition of the bimetallic nanoparticles corresponds to the formula $Fe_{12}Ni_{36}$, exhibiting a cubic structure. The empirical formula for these nanoparticles is $FeNi_3$. The XRD analysis also confirmed the presence of a cubic unit cell in the Fe/Ni bimetallic nanoparticles. The bond angle between iron and nickel atoms is 135.2245°, and the bond length between iron and nickel atoms is 2.45923 Å, with a bond ratio of 1:3 (Fe:Ni). The polyhedral structure of the Fe/Ni bimetallic nanoparticles reveals two distinct bond lengths: 2.75567 Å at the center of the cubic structure and 2.56865 Å at the base of the structure. This indicates that the bond distance is largest in the middle of the structure and smallest near the periphery. The structure also exhibits a dihedral angle of 64.8645°. In the unit cell of the Fe/Ni bimetallic nanoparticles, the polyhedral structure contains 225 bonds, associated with the configuration labeled as "535". The cubic shape of the Fe/Ni nanoparticles is consistently confirmed by XRD analysis. Moreover, various other configurations with different symmetries also exhibit cubic structures. Therefore, XRD characterization plays a crucial role in nanotechnology research, as it provides valuable information about the geometry, structure, and morphology of nanoparticles, which are essential for understanding and optimizing their properties.

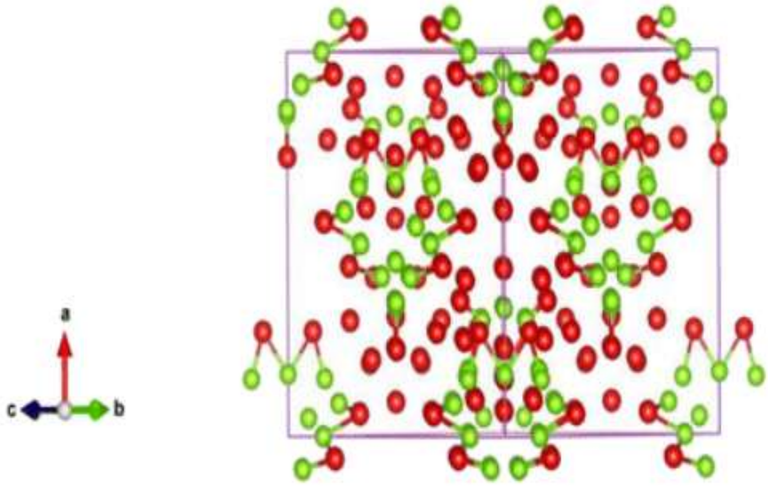

Figure 2 Cubic Morphology of Fe/Ni Bimetallic Nanoparticles

SEM Analysis

The results of the scanning electron microscopy (SEM) provide information on the size, shape, morphology, and porosity of the nanoparticles. Various scanning electron micrographs (SEMs) of the bimetallic Fe/Ni nanoparticles at various magnifications are shown in Figure 3. The scanning electron microscopy results in Figure 3a and 3b reveal that the nanoparticles' surfaces have combined, and that a majority of the nanoparticles exhibit an uneven shape and size within the 50 µm range. Some nanoparticles are within the 100 nm range, as seen in Figure 3c. At a higher magnification, the nanoparticles' rough edges may be seen in Figure 3c. The attraction forces of the wandering wall between the bimetallic nanoparticle particles are what cause them to stick together. The aggregates in the photographs stand out because of this.

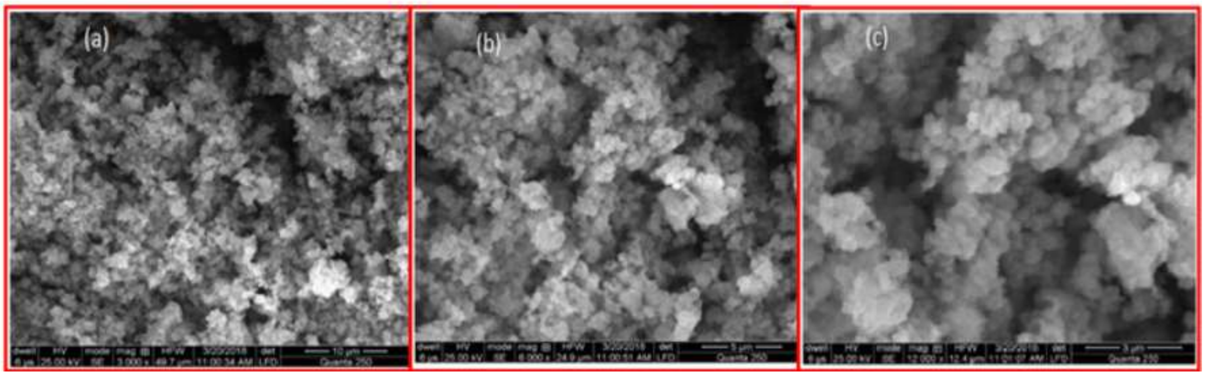

Figure 3 SEM Images of Synthesized Fe/Ni Bimetallic Nanoparticles at Different Magnifications (a–c)

The presence of bimetallic nanoparticles on the surfaces of the product's big aggregates is seen in Figure 3c. The bimetallic nanoparticles' very small size. Uncertain and irregularly shaped, bimetallic nanoparticles are what we have here.

TEM Analysis

We can learn a lot about the shape, size, and chemical composition of the nanoparticles from the data provided by transmission electron microscopy (TEM). Pictured at various magnifications in Figure 4 are transmission electron micrographs of bimetallic nanoparticles. Figure 4 shows that the size of the nanoparticles varies and that the majority of them have an irregular shape. The nanoparticles' roughness at the corners is clearly seen in Figure 4. Figure 4 shows that the majority of nanoparticles are larger than 100 nm. Particles smaller than 100 nm are also detected. At various magnifications, the nanoparticles' nanometre-range size was seen. The size of bimetallic nanoparticles may be altered by a number of factors, including manufacturing methods, structure, reduction agent, temperature, pH, and duration. The surface roughness's of these nanoparticles are seen in the TEM photographs. Because of the deep hues of the light, the hollow shape of these particles stands out.

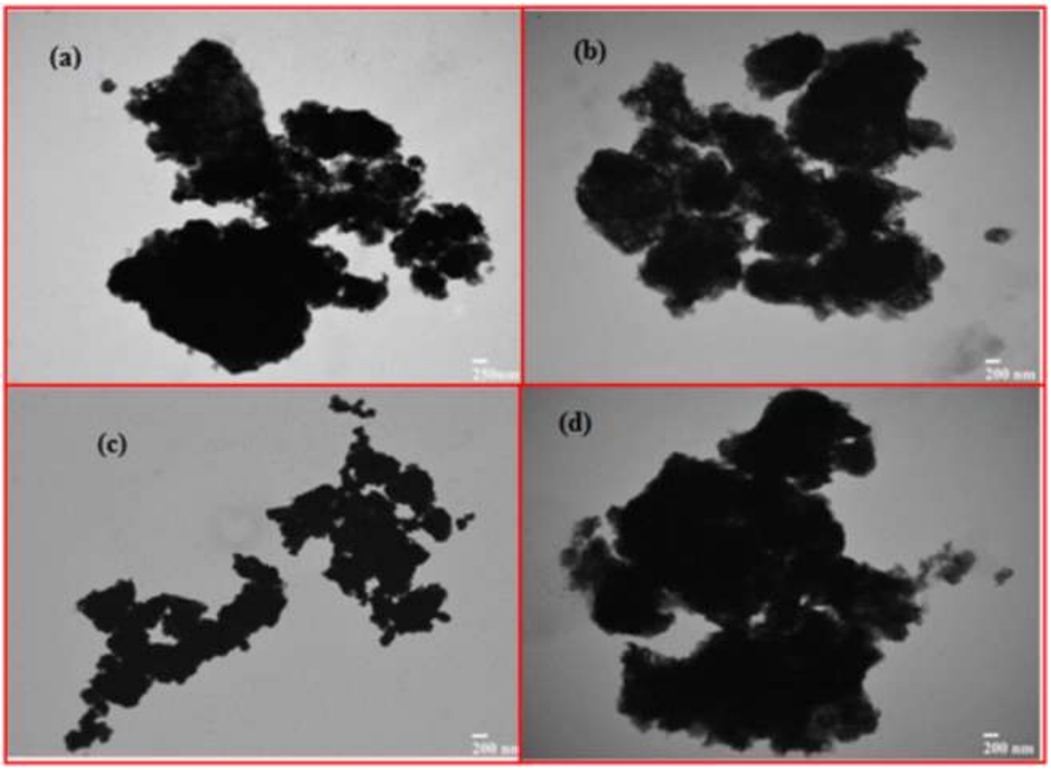

Figure 4 TEM Images of Synthesized Fe/Ni Bimetallic Nanoparticles Showing Different Aggregation States (a–d)

Physicochemical Properties

Both the cloud point and the pore point... A second-order quadratic equation was used to fit the experimental data. The data distribution was found to be good in the regression analysis, with an R2 value of 0.8364 for cloud point and an R2 value of 0.8364 for the other variables. At certain concentrations, pure kerosene fuel has higher pour and cloud points than additive kerosene fuel. With a little drop at the outset, the cloud point and pour point values begin to rise with increasing concentrations of bimetallic nano catalyst. Figure 5 shows that the addition of a bimetallic nano catalyst does not significantly affect the cloud point or the pouring point.

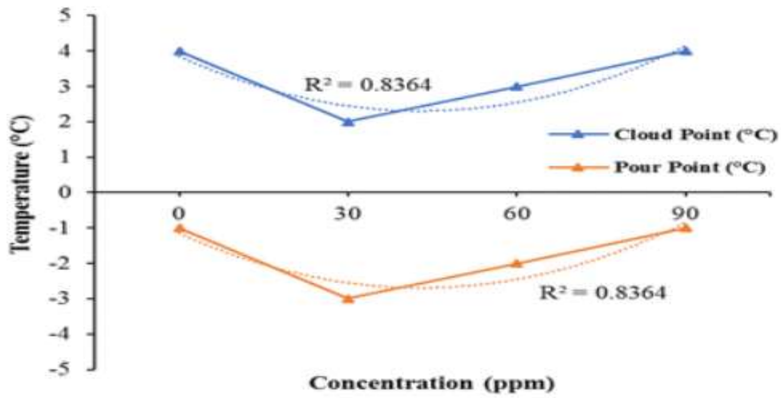

Figure 5 Influence of Fe/Ni Bimetallic Nanoparticles on the Pour Point and Cloud Point of Kerosene Oil

The values of the pour point and cloud point are almost identical to those of pure kerosene fuel. The addition kerosene fuel's cloud point and flame point, which are characteristics that are affected at low temperatures, have not been much altered. According to Figure 7. This means that the bimetallic nano catalyst isn't very useful.

Viscous Flow Property

The results of the experiments were analyzed using linear regression. Figure 6's graph shows that the data is correctly aligned in a linear pattern, with an R2 value of 0.9169.

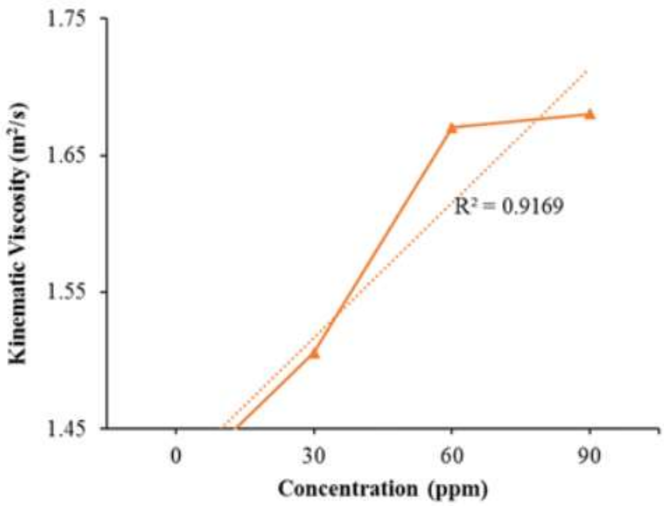

Figure 6 Influence of Fe/Ni Bimetallic Nanoparticles on the Kinematic Viscosity of Kerosene Fuel

The blend's kerosene oil and additive nanoparticles' viscosity as determined by a viscosity meter. At room temperature, the viscosity of each sample was measured. The specific surface area per unit time for pure kerosene fuel is 1.4078 m2 s−1. The difference in viscosity between the nano catalyst at different concentrations and the pure kerosene gas. A linear relationship exists between the concentration of nano catalysts and the kerosene fuel viscosity. Viscosity vs. different concentrations is seen in Figure 6.

Increasing the concentration of the Fe/Ni bimetallic nano catalyst considerably increases the viscosity of natural kerosene. The sample's viscosity is much greater when the nano catalyst concentration is high. So, boosting the fuel's viscosity with a little amount of the nano catalyst is very efficient. Increasing the fuel's viscosity improves engine efficiency. Consequently, bimetallic nano catalysts made of iron and nickel are very useful for enhancing fuel economy. Fuel with a higher viscosity provides better lubrication, leading to less turbulent flow. The reduced flow rate of the modified kerosene fuel in comparison to the pure fuel indicates that the modified fuel is thicker than the pure fuel, which in turn increases resistance between layers and reduces fuel turbulence. This results in a significant improvement in the engine's efficiency. Therefore, the very little number of bimetallic nanoparticles is highly beneficial for increasing the kerosene fuel's viscosity and therefore its efficacy.

Density Ratio

After plugging the experimental data into a second-order quadratic equation, regression analysis proved that the data followed the expected distribution (R2 = 0.9657). Using a specialized gravity meter, the specific gravities of pure kerosene oil and modified kerosene oil were determined. As shown in Figure 8, the particular gravities of the two fuels are significantly different. Increasing the concentration of the bimetallic nano catalyst leads to an improvement in the specific gravity values. The effect of the nano catalyst's minute amount on the kerosene fuel's specific gravity is shown at 90 ppm, which signifies peak specific gravity compared to the other lowered concentrations. Fuel with a higher specific gravity will run the engine more efficiently. The bimetallic Fe/Ni nano catalyst, even at a very small dose, significantly improves the efficiency of the kerosene fuel by increasing the gas's specific gravity.

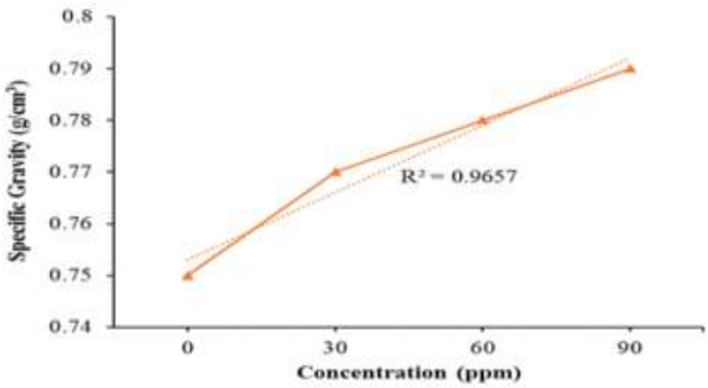

Figure 7 Influence of Fe/Ni Bimetallic Nanoparticles on Kerosene Fuel Specific Gravity

Energy Content Analysis

In Figure 8, we can see the calorimetric data for both the untreated natural kerosene oil and the Fe/Ni bimetallic nano catalyst at different doses. The calorie content of pure kerosene oil is much lower than that of the modified kerosene kind. With an R2 of 0.7725, linear regression analysis proved that the data followed a normal distribution.

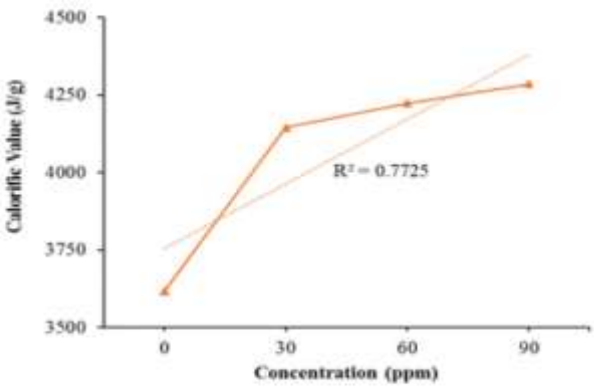

Figure 8 Calorimetric Analysis of Natural Kerosene Oil with Varying Dosages of Fe/Ni Bimetallic Nano catalyst

Increasing the concentration of the bimetallic nano catalyst leads to a linear improvement in the calorific values. Therefore, the bimetallic nanoparticles significantly affect the calorific values of kerosene fuel, as can be shown in Figure 8. Fuels made from modified kerosene and pure kerosene have very different calorific values. A higher calorific value is indicative of a sample with a higher concentration of bimetallic nanoparticles. This means that the kerosene fuel was much more effective after adding bimetallic nanoparticles.

UV–Vis Spectra of Dyes

The UV-visible spectra of methylene blue solutions with varying concentrations of color, measured in the absence of a catalyst, are shown in Figure 9. At 663.5 nm, the maximum absorption for 10 ppm, 15 ppm, and 20 ppm is 2.317, 2.932, and 3.412, respectively. Based on these numbers, it's clear that increasing the dye concentration significantly boosts the absorption value. A concentration of 20 ppm of nano catalyst and H2O2 was selected for the exploration of supplementary parameters. Our everyday encounters with high concentration dye degradation led us to choose this particular job's enhanced concentration of dye. The wastewater from the majority of businesses contains high amounts of these organic pigments. The wastewater from most companies contains high concentrations of these organic dyes.

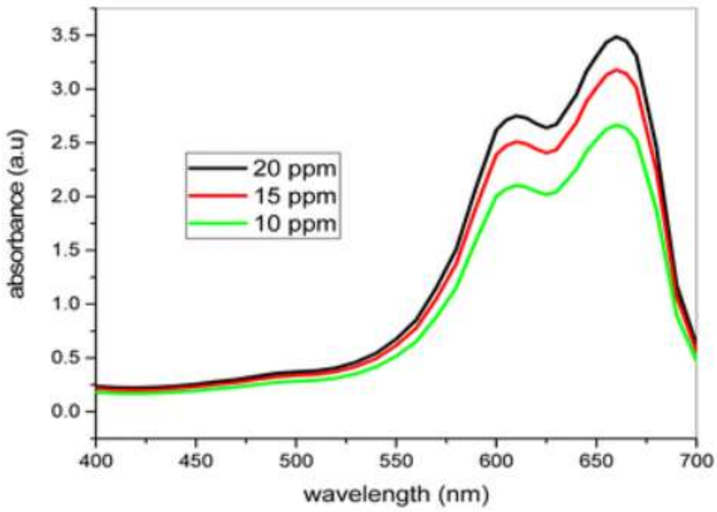

Figure 9 Effect of Dye Concentration on Absorbance Without Catalyst

Catalyst-Free Dye Degradation Studied by UV–Vis Spectroscopy

The product degrades in the presence of 2 ml of H2O2 without a catalyst, as seen in Figure 10. The figure clearly shows that the rate of degradation of the methylene blue dye was very sluggish; the dye remained undissolved even after 60 minutes of stirring in sunshine. Consequently, the catalyst plays a crucial role in the quick methylene blue dye breakdown process. The deterioration was only completed in 60 minutes, at a rate of 10–20%. So, it's almost hard to degrade colours without a catalyst. Due to the fact that 2 ml of H2O2 only partially decomposed the methylene blue dye, it is not only possible to breakdown all organic dyes using H2O2. Degradation of organic dyes is facilitated by the bimetallic nano catalyst. Because these organic colours are present in the wastewater of many different types of businesses, getting them out is crucial.

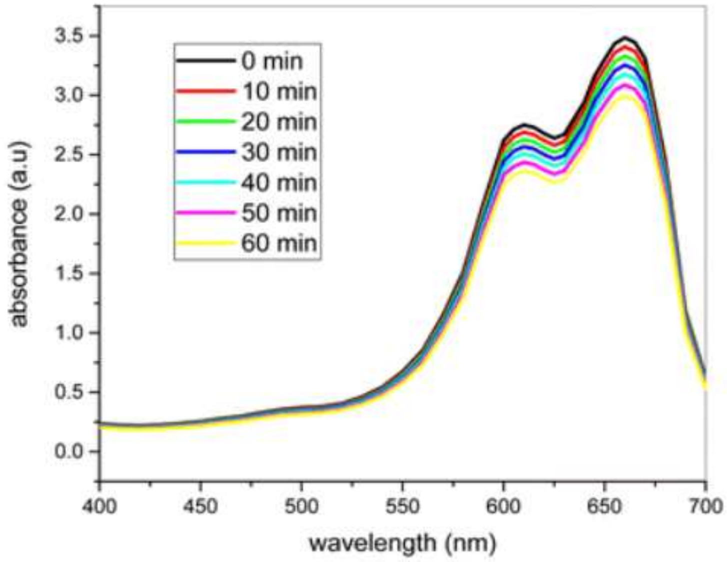

Figure 10 Sunlight-Induced Dye Degradation Over Time Without Catalyst (Dye: 20 ppm, H_2O_2: 2 mL)

5. CONCLUSION

Hydrothermal treatment was used to effectively prepare and increase the performance of superparamagnetic iron oxide nanoparticles (SPIONs) for use in magnetic hyperthermia applications. For effective heat production when subjected to an alternating magnetic field, the hydrothermal process is vital, as it helps generate nanoparticles with greater size uniformity, higher crystallinity, and enhanced magnetic characteristics. of the increased specific absorption rate (SAR), it was found that smaller dosages of nanoparticles may be employed to reach the therapeutic temperature that was sought, which might lead to a decrease in adverse effects. Hydrothermally treated SPIONs showed promise as potential candidates for use in cancer therapy by magnetic hyperthermia, according to the research. To determine their actual therapeutic use, further studies, including as in vivo trials and safety assessments, are required. This study adds to the growing body of evidence that supports the need for less intrusive, more effective, and safer cancer treatments.

REFERENCES

1) C. Pucci, A. Degl'Innocenti, M. B. Gümüş, and G. Ciofani, "Superparamagnetic iron oxide nanoparticles for magnetic hyperthermia: Recent advancements, molecular effects, and future directions in the omics era," *Biomater. Sci.*, vol. 10, no. 9, pp. 2103–2121, 2022.
2) S. R. Ansari, N.-J. Hempel, S. Asad, P. Svedlindh, C. A. S. Bergström, K. Löbmann, and A. Teleki, "Hyperthermia-Induced in Situ Drug Amorphization by Superparamagnetic Nanoparticles in Oral Dosage Forms," *ACS Appl. Mater. Interfaces*, vol. 14, no. 19, pp. 21978–21988, 2022.
3) M. Coïsson, G. Barrera, F. Celegato, P. Allia, and P. Tiberto, "Specific Loss Power of Magnetic Nanoparticles: A Machine Learning Approach," *APL Mater.*, vol. 10, no. 8, Art. no. 081108, 2022.
4) S. Savliwala, A. Chiu-Lam, M. Unni, A. Rivera-Rodriguez, E. Fuller, K. Sen, M. Threadcraft, and C. Rinaldi, "Magnetic Nanoparticles," in *Nanoparticles for Biomedical Applications*, Elsevier, vol. 5, no. 1, pp. 195–221. 2020,
5) J. Dulińska-Litewka, A. Łazarczyk, P. Hałubiec, O. Szafrański, K. Karnas, and A. Karewicz, "Superparamagnetic iron oxide nanoparticles—Current and prospective medical applications," *Materials*, vol. 12, no. 4, Art. no. 617, 2019.
6) J. Pala, M. Moradiya, C. Savaliya, and J. Markna, "Tailoring of magnetic hyperthermia treatment using superparamagnetic iron oxide nanoparticles," *MOJ Biol. Med.*, vol. 2, no. 1, pp. 174–175, 2017.
7) Y. Lv, Y. Yang, J. Fang, et al., "Size dependent magnetic hyperthermia of octahedral Fe3O4 nanoparticles," *RSC Adv.*, vol. 5, no. 94, pp. 76764–76771, 2015.
8) A. E. Deatsch and B. A. Evans, "Heating Efficiency in Magnetic Nanoparticle Hyperthermia," *J. Magn. Magn. Mater.*, vol. 354, no. 3, pp. 163–172, 2014.
9) K. D. Bakoglidis, K. Simeonidis, D. Sakellari, G. Stefanou, and M. Angelakeris, "Size-Dependent Mechanisms in AC Magnetic Hyperthermia Response of Iron-Oxide Nanoparticles," *IEEE Trans. Magn.*, vol. 48, no. 4, pp. 1320–1323, 2012.
10) D. Ho, X. Sun, and S. Sun, "Monodisperse magnetic nanoparticles for theranostic applications," *Acc. Chem. Res.*, vol. 44, no. 1, pp. 875–882, 2011.
11) S. Laurent, S. Dutz, U. O. Häfeli, and M. Mahmoudi, "Magnetic Fluid Hyperthermia: Focus on Superparamagnetic Iron Oxide Nanoparticles," *Adv. Colloid Interface Sci.*, vol. 166, no. 1–2, pp. 8–23, 2011.
12) A. Avram, A. Radoi, V. Schiopu, et al., "Synthesis and characterization of γ-Fe2O3 nanoparticles for applications in magnetic hyperthermia," *Synthesis*, vol. 10, P151, 2011.
13) M. Kallumadil, M. Tada, T. Nakagawa, M. Abe, P. Southern, and Q. A. Pankhurst, "Suitability of commercial colloids for magnetic hyperthermia," *J. Magn. Magn. Mater.*, vol. 321, no. 2, pp. 1509–1513, 2009.
14) S. Laurent, D. Forge, M. Port, A. Roch, C. Robic, L. Vander Elst, and R. Muller, "Magnetic iron oxide nanoparticles: Synthesis, stabilization, vectorization, physicochemical characterizations and biological applications," *Chem. Rev.*, vol. 108, no. 1, pp. 2064–2110, 2008.